SUPPLEMENTARY MATERIAL

Eyring diffusivity

The melt viscosity of AND1 was calculated using the model of Giordano et al. (2008) for non-Arrhenian multicomponent silicate melts which is based on the Vogel-Fulcher-Tammann (VFT) equation (Vogel, 1921; Fulcher, 1925; Tammann and Hesse, 1926):

$$\log\eta = A + [B/(T – C)] \qquad \text{(Eq. A1)}$$

where η is the viscosity of the melt in Pa s; A, B, and C are adjustable parameters (see Giordano et al., 2008, for details); and T is the temperature in K. The predicted viscosity obtained for AND1 is 2.19 Pa s at 1698 K (i.e., at the temperature of the N diffusion experiments, 1425°C).

The Eyring diffusivity is compared to nitride diffusion in AND1 melt in Figure A2. The diffusivity of network formers (Si, Al) and O^{2-} at 1698 K (i.e., 1425 °C) is $\sim 3.6 \times 10^{-7}$ cm^2 s^{-1}, whereas the diffusion coefficient for nitride is on the order of $5.3 \pm 1.5 \times 10^{-8}$ cm^2 s^{-1} (Fig. A2).

### Carbon and water content of sample AND1

CO_2 and H_2O concentrations along profile A in sample AND1 (1 atm, 1425 °C, 3 h, IW –8) were measured using the Cameca IMS-1270 E7 ion microprobe at the Centre de Recherches Pétrographiques et Géochimiques (Nancy, France). A Cs$^+$ primary beam was used with a current of 0.5 nA accelerated at 10 kV and a raster of 5×5 μm. Standards and samples were pre-sputtered for 180 s over an area of 10×10 μm with a primary beam current of 2 nA to remove any traces of contaminant carbon and hydrogen from the surface. For analyses, the beam was focused to a spot of 5 to 10 μm diameter. The $^{12}C^-$, $^{16}O^1H^-$, $^{18}O^-$, and $^{30}Si^-$ signals were collected in peak-jumping mode on an electron multiplier for 10 cycles. We used a mass resolution (m/Δm) of 7000 to separate masses $^{17}O^-$ and $^{16}O^1H^-$. Concentrations were obtained using a set of natural basaltic glass standards with known CO_2 and H_2O contents as calibrants (Moussalam et al., 2019). The major element composition of these standards is comparable to that of AND1 (e.g., $SiO_2 \sim 50$ wt.%; see Moussalam et al., 2019 for more information on the standards). Based on the reproducibility of the count rates over 10 cycles and the standard signals, maximum uncertainties on the carbon and water contents are 12% and 24%, respectively.

Along profile A, from the surface of the glass cylinder towards the center, measured carbon (equivalent CO_2) concentrations range from 465 ± 49 to 172 ± 15 ppm (Fig. A3). The plateau with concentrations of ~ 200 ppm CO_2 at ~ 500–2100 μm depth may be due to the dissolution of carbon into the melt during incremental filling of the compacted graphite tube with the starting material prior to the diffusion experiments. The second plateau (i.e., 400–500 ppm equivalent CO_2), close to the gas-melt interface, was likely formed during the diffusion experiment at $fO_2 = $ IW –8, $T = 1425$°C, and using a CO-N$_2$ gas mixture, as a result of inward diffusion of carbon. Experiments at high
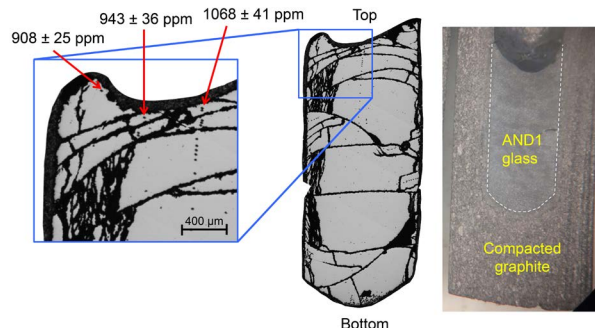

FIGURE A1: N content of the glass AND1 (1 atm, 1425 °C, 3 h, IW –8) at three different locations along the gas-melt interface. The picture on the right shows the AND1 glass in the compacted graphite crucible (the dashed white line delimits the contact between the compacted graphite and the glass).
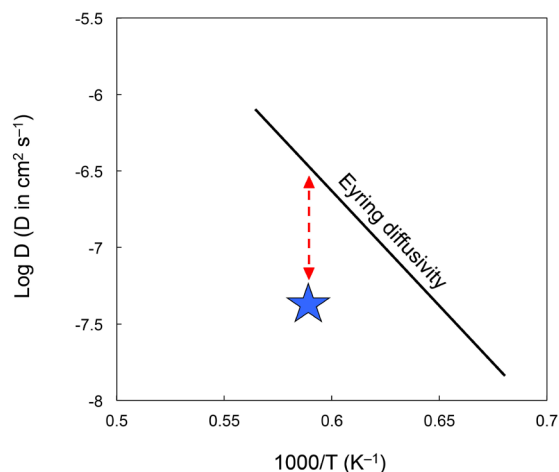
FIGURE A2: Comparison of the N^{3-} diffusivity obtained for AND1 (blue star) at 1698 K (1425°C) with the Eyring diffusivity for basaltic andesite melts (see text for details on the calculation).

pressure and under reducing conditions indicate that carbon can be present in the form of various species in silicate melts (e.g., C-N, C^{4+}, C-O, and/or C-H; Dalou et al., 2019; Grewal et al., 2020). However, the C-N vibration band was not observed by Raman spectroscopy in N-rich MO2 glass (6002 ± 91 ppm), synthesized and equilibrated under similar conditions as AND1 (Boulliung et al., 2020).

The presence of 531 ± 52 to 217 ± 51 ppm equivalent H_2O in the quenched glass (Fig. A3) indicates that conditions were not completely anhydrous during the diffusion experiments and/or during the melt synthesis, suggesting that hydrogen may form C-H and/or N-H complexes. However, under these highly reduced conditions, N-H complexes are expected to represent a minor N-bearing species (Grewal et al., 2020), and no N-H vibration bands were detected by Raman spectroscopy in the N-rich MO2 glass (6002 ± 91 ppm) (Boulliung et al., 2020).
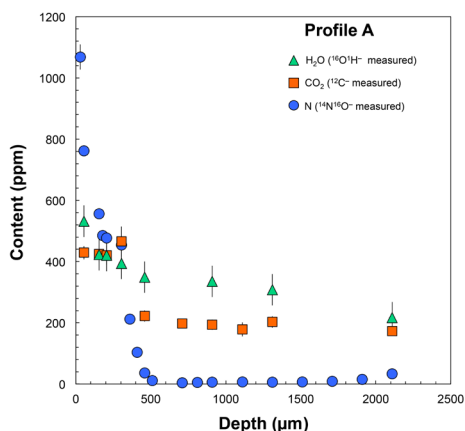
FIGURE A3: H_2O, CO_2, and N content as a function of depth along profile A in sample AND1 (1 atm, 1425 °C, 3 h, IW –8).

REFERENCES CITED

Boulliung, J., Füri, E., Dalou, C., Tissandier, L., Zimmermann, L., and Marrocchi, Y (2020) Oxygen fugacity and melt composition controls on nitrogen solubility in silicate melts. Geochimica et Cosmochimica Acta, 284, 120-133.

Dalou, C., Hirschmann, M.M., Jacobsen, S.D., and Le Losq, C. (2019) Raman spectroscopy study of COHN speciation in reduced basaltic glasses: Implications for reduced planetary mantles. Geochimica et Cosmochimica Acta 265, 32–47.

Fulcher, G.S. (1925) Analysis of recent measurements of the viscosity of glasses. Journal of the American Ceramic Society, 8(6), 339-355.

Giordano, D., Russell, J.K., and Dingwell, D.B. (2008) Viscosity of magmatic liquids: a model. Earth and Planetary Science Letters, 271(1-4), 123-134.

Grewal, D.S., Dasgupta, R., and Farnell, A. (2020) The speciation of carbon, nitrogen, and water in magma oceans and its effect on volatile partitioning between major reservoirs of the Solar System rocky bodies. Geochimica et Cosmochimica Acta.

Moussallam, Y., Rose-Koga, E.F., Koga, K.T., Médard, E., Bani, P., Devidal, J.L., and Tari, D. (2019) Fast ascent rate during the 2017–2018 Plinian eruption of Ambae (Aoba) volcano: a petrological investigation. Contributions to Mineralogy and Petrology, 174(11), 90.

Tammann, G.H.W.Z., and Hesse, W. (1926) Die Abhängigkeit der Viscosität von der Temperatur bie unterkühlten Flüssigkeiten. Zeitschrift für anorganische und allgemeine Chemie, 156(1), 245-257.

Vogel, D.H. (1921) Temperaturabhängigkeitsgesetz der Viskosität von Flüssigkeiten. Physik Z, 22, 645-646.